Imaging

6

Daisuke Kawamura

Abstract

Since the first report by Robert Kienböck himself, the diagnosis of Kienböck's disease has usually been made on plain radiographs. Radiographs show different lunate findings as the disease progresses. In early lesions, the lunate shows a normal architecture and bone density, whereas as the disease progresses, it shows osteosclerosis, fragmentation of the lunate, and abnormal carpal arrangement. Radiographs are also important in determining the associated anatomic and mechanical properties of the involved wrist, such as ulnar variance, radial inclination, carpal height, radioscaphoid angle, and lunate size or shape.

Magnetic resonance imaging (MRI) is helpful early in the disease when plain radiographs may not reveal any abnormalities. On T1-weighted images, the lunate demonstrates diffuse low signal intensity as a result of decreased vascularity. T2-weighted images may reveal high or low signal intensity, depending on the extent of the disease process. It is critical to consider that this diffuse signal change within the entirety of the lunate is necessary to establish the diagnosis of Kienböck disease.

Computed tomography (CT), especially sagittal reconstruction views, is helpful in assessing the extent of articular surface collapse and the presence of fractures. CT sagittal views are also helpful in detecting the presence of carpal instability as well as early osteoarthritis of the radiocarpal and midcarpal joints.

Staging of Kienböck disease depends primarily on the radiographic findings. Staging is an important step for planning the treatment by the stage of disease. The classification system described by Lichtman et al. is used most commonly.

D. Kawamura (✉)
Department of Orthopaedic Surgery, Faculty of Medicine and Graduate School of Medicine, Hokkaido University, Sapporo, Hokkaido, Japan
e-mail: dkawa@pop06.odn.ne.jp

N. Iwasaki (ed.), *Introduction to Kienböck's Disease*,
https://doi.org/10.1007/978-981-19-8375-7_6

Keywords

Imaging · Radiography · Magnetic resonance imaging · Staging

6.1 Standard Radiographs

Robert Kienböck, a radiologist, published his renowned article "Über traumatische Malazie des Mondbeines und ihre Folgezustände: Entartungsformen und Kompressionsfrakturen," which appeared in Fortschritte auf dem Gebiet der Roentgenstrahlen in 1910 [1]. The article presented 16 cases showing "traumatic malacia of the lunate," including clinical and radiographic findings. This article was published only 13 years after the discovery of X-rays by Conrad Roentgen, and since then, the diagnosis of Kienböck's disease has usually been made on plain radiographs.

Radiographs show different lunate findings as the disease progresses. In early lesions, the lunate shows a normal architecture and bone density, whereas as the disease progresses, it shows osteosclerosis, fragmentation of the lunate, and abnormal carpal arrangement.

A diligent search should be performed for evidence of compression fracture or changes in the relative density of the lunate in patients with acute or chronic wrist pain. Radiographs are also important in determining the associated anatomic and mechanical properties of the involved wrist, such as ulnar variance, radial inclination, carpal height, radioscaphoid angle, and lunate size or shape. First, obtaining adequate posteroanterior (PA) radiographs of the wrist is important for accurate and reproducible measurements. Lichtman et al. emphasized the importance of taking adequate radiographs in their article describing the use of the Lichtman classification [2] in the measurement of ulnar variance changes with forearm rotation, wrist deviation, and the X-ray beam incidence angle [3–6].

A standard PA radiograph is taken with standard positioning of the arm; the wrist and the forearm are in the neutral position, the elbow flexed 90°, and the shoulder abducted to 90° [3]. Typical measurements and their clinical significance are described below.

6.1.1 Ulnar Variance

Since Hulten's report in 1928, the association between negative ulnar variance and Kienböck's disease has been investigated. Several methods are used to measure ulnar variance (Fig. 6.1).

Gelberman et al. measured ulnar variance using the so-called "project a line technique [7], in which a line is drawn from the ulnar side of the articular surface of the distal radius toward the ulna (Fig. 6.1a). The variance is defined as the distance between the line and the distal end of the ulna. Although several authors have followed this technique [8], anatomical landmarks to draw the line were not described in the original article by Gelberman.

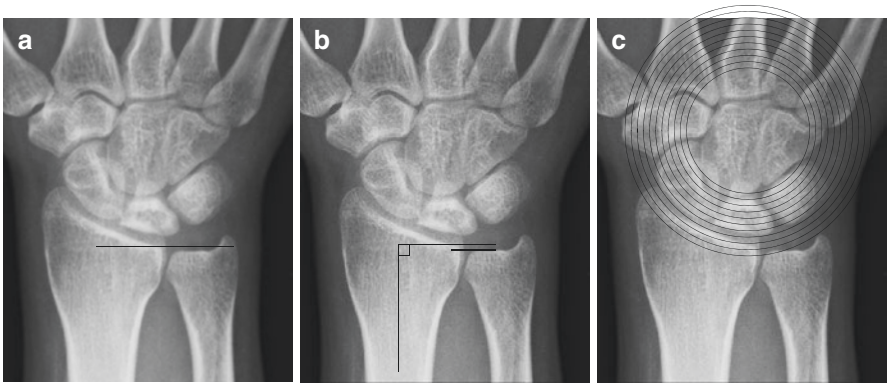

Fig. 6.1 Methods of ulnar variance measurements. (**a**) The project a line technique, (**b**) Method of perpendiculars, (**c**) Concentric circle technique

Coleman et al. reported another method in [9]; this method involves drawing a line perpendicular to the longitudinal axis of the radius through the distal ulnar aspect of the radius, following which the distance between the line and cortical rim of the ulnar head is measured (Fig. 6.1b).

Palmer et al. reported ulnar variance measurement with a transparent plastic template marked with concentric semicircles of varying radii [10]. The template had a selection of radii ranging from 20 to 50 mm in 1-mm increments. The template curve that most closely approximated the concavity of the distal radial sclerotic line was chosen. The number of radii separating this template from the cortical rim of the ulnar head represents the amount of ulnar variance in millimeters.

Yoshida et al. modified Palmer's measurement [11] by using the circumferential template to the lunate fossa of the radius and not to the whole distal joint surface of the radius (Fig. 6.1c).

Steyers et al. compared the three methods of measuring ulnar variance [12] and found all of them to be highly reliable. These findings suggest that the technique may be selected at the discretion of the clinician when measuring ulnar variance.

Several authors have highlighted that ulnar variance differs between males and females and increases with advancing age [5, 13]. Studies have also reported an association between negative ulnar variance and Kienböck's disease [7, 14, 15], although several other studies have rejected this hypothesis [4, 5, 16, 17].

6.1.2 Radial Inclination

The radial inclination was measured as the angle between a line from the ulnar side of the carpal surface of the radius to the tip of the radial styloid and a line perpendicular to the axis of the radius or the ulna [8, 18].

Some authors claim that a flatter radial inclination may predispose individuals to Kienböck's disease [8, 18]. Mirabello et al. reported a correlation between the slope of the distal radial articular surface and the age of onset [19].

6.1.3 Carpal Height Ratio

The Carpal Height Ratio (CHR) is calculated as the distance from the proximal end of the third metacarpal to the radial articular surface divided by the length of the third metacarpal [20]. The CHR declines in advanced stages after Lichtman IIIb, suggesting the presence of carpal instability.

6.1.4 Radioscaphoid Angle

The long axis of the scaphoid is determined with a line tangential to the palmar outline of the scaphoid using the technique of Gilula and Weeks from the lateral view of the wrist radiographs [21]. The axis of the radius is determined by a dorsal cortex line through the radius or drawn through the center of the radius at 2 and 5 cm proximal to the joint [18, 22]. Condit et al. found that the preoperative radioscaphoid angle correlated best with clinical outcomes [23].

6.1.5 Size or Shape of the Lunate

Together with ulnar variance and radial inclination, lunate morphology is also considered to be a mechanical factor of Kienböck's disease. Several reports have described that the height and diameter of the lunate are smaller in patients with Kienöck's disease than in normal controls [8, 18]. It is presumed that these anatomical features may result in greater load transmission onto the lunate, which may lead to avascular necrosis.

Antuno-Zapico classified lunates into three types according to the angle between the lateral scaphoid and the proximal radial sides of the lunate (Fig. 6.2) [24]. In type I, the angle is more than 130° (Fig. 6.2a); in type II, the angle is approximately 100° (Fig. 6.2b); and in type III, there are two distinct facets on the proximal surface that articulate with the radius and the triangular fibrocartilage (Fig. 6.2c). Antuno-Zapico described the association of ulnar negative variance in wrists with type I lunate and ulnar neutral or positive variance in type II and III lunates and theorized that type I lunates are the weakest to compressive stress.

Viegas et al. classified lunate morphology into two types based on the absence (type I) (Fig. 6.2d) or presence (type II) of a medial hamate facet (Fig. 6.2e) [25]. Ulnar variance, age, sex, and side were not correlated with the presence or absence of a medial hamate facet on the lunate.

Tatebe et al. reported that the prevalence of type 2 lunate in Kienböck's disease was much lower (28%) than that described in the report by Viegas et al. (65.5%) [26]. They presented data implying a relationship between the lunate type and Kienböck's disease. In contrast, Tsuge et al. reported that the medial facet was

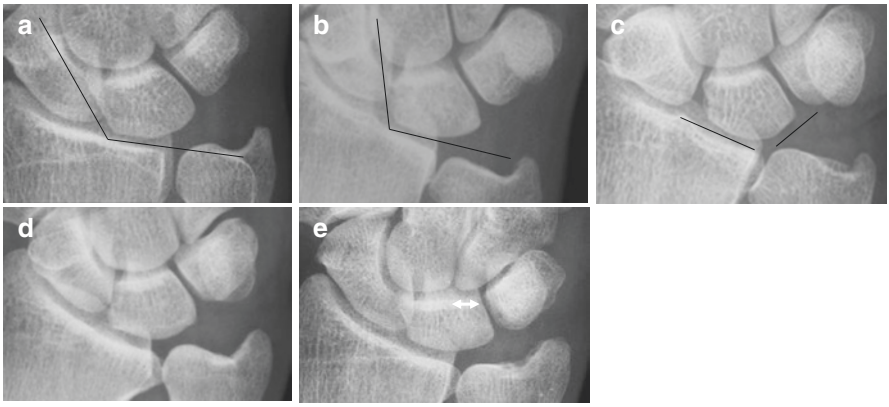

Fig. 6.2 Classification of lunate morphology. (**a**–**c**) Morphologic classification by Antuno-Zapico, (**a**). Type I, (**b**) Type II, (**c**) Type III. (**d**, **e**) Morphologic classification by Viegas, (**a**) Type I, (**b**) Type II (white arrow: medial facet)

present in 37% of the Kienböck group and 42% of the normal controls; however [18], there was no significant difference between the two groups in terms of the incidence of this medial facet.

Rhee et al. studied the effect of lunate type on the radiographic characteristics of patients with Kienböck's disease [27]. They concluded that lunate morphology may affect the severity of Kienböck's disease at the time of initial presentation. Type II lunates appear to be protective against coronal and scaphoid flexion deformities.

6.2 Magnetic Resonance Imaging

Magnetic Resonance Imaging (MRI) is helpful early in the disease when plain radiographs may not reveal any abnormalities. On T1-weighted images, the lunate demonstrates diffuse low signal intensity as a result of decreased vascularity. T2-weighted images may reveal high or low signal intensities depending on the extent of the disease process. It is critical to consider that this diffuse signal change within the entirety of the lunate is necessary to establish a diagnosis of Kienböck's disease (Fig. 6.3c, f, i). Other pathologic conditions, such as ulnocarpal abutment (in which the pathology is limited to the proximal ulnar aspect of the lunate), fractures, and tumors, demonstrate abnormal signals localized to a specific area.

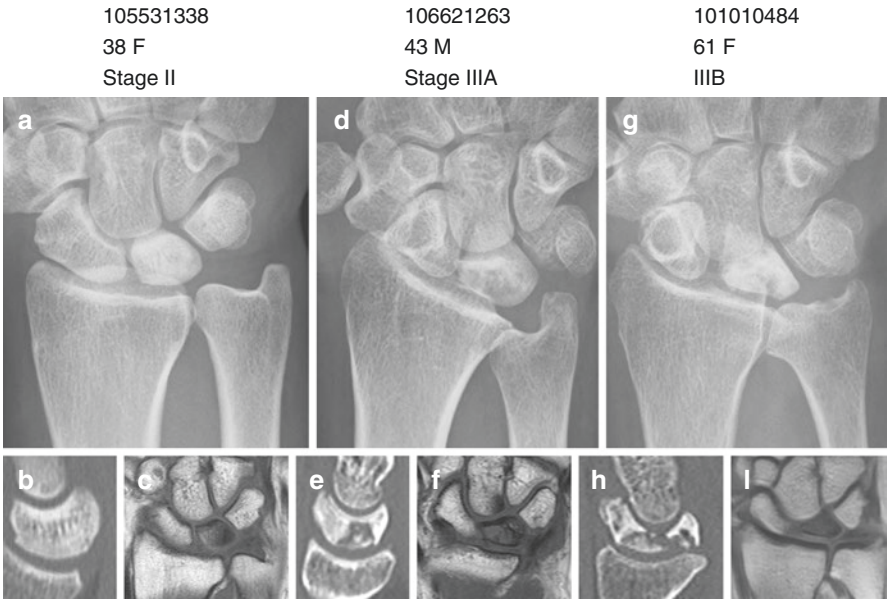

Fig. 6.3 Typical imaging findings of Kienböck's disease. (**a**–**c**) A 38-year-old woman with stage II disease. (**d**–**f**) A 43-year-old man with stage IIIA disease. (**g**–**i**) A 61-year-old woman with stage IIIB disease. (**a**, **d**, **g**) plain radiographs. (**b**, **e**, **h**) Sagittal reconstruction views of computed tomography, (**c**, **f**, **i**) T1-weighted images of magnetic resonance imaging)

6.3 Computed Tomography

Computed Tomography (CT), especially sagittal reconstruction views, is helpful in assessing the extent of articular surface collapse and the presence of fractures (Fig. 6.3b, e, h). CT sagittal views are also helpful in detecting the presence of carpal instability as well as early osteoarthritis of the radiocarpal and midcarpal joints.

Friedman et al. reported that direct coronal CT of the wrist is more sensitive than plain radiographs [28].

Schmitt et al. found that 24 out of 37 patients had a higher stage on CT than on radiographs. CT enables earlier and more extensive detection of cystic lesions in the lunate or shell-formed fractures at the proximal pole of the lunate [29].

Mohan et al. measured the width and height ratio of the lunate in the sagittal planes on a CT scan [30]. They reported that the width/height ratio correlates with carpal height and found that lunate collapse precedes the reduction in the carpal height ratio in some patients and concluded that this ratio is a better measure of lunate collapse.

6.4 Staging

Staging or classification is an important step in the evaluation of patients with Kienböck's disease because structural and kinematic alterations appear to have a significant effect on treatment outcomes. Furthermore, staging is important for accurately comparing the clinical results of different treatment options. The surgical management options for Kienböck's disease are dictated by the disease stage.

Ståhl described a radiographic and pathologic classification system for Kienböck's disease in 1947 [31]. Decoulx et al. also proposed his renowned classification system in 1957 [32]. Lichtman et al. modified Stahl's original classification in 1977 [2]. The classification scheme described by Lichman et al. is most widely used and has evolved with time [33–35]. This classification system is based on radiographic and clinical findings rather than on surgical or pathologic examination of the lunate (Table 6.1).

Lichtman's first classification in 1977 was composed of four stages according to the structural alteration of the lunate and the surrounding carpal bones. Stage I indicates normal architecture and density of the lunate on plain radiographs. A linear fracture line in the lunate may be present, but lunate collapse is not observed. In an original article in 1977, Lichtman stated that a bone scan may be abnormal in stage I disease. However, it has fallen out of favor since the introduction of MRI. MRI is an ideal imaging technique for stage I. Uniformly decreased signal intensity in both T1- and T2-weighted images in comparison with the neighboring bones reflects the loss of vascularity. An increased signal on T2 may represent revascularization [35].

In stage II, the lunate demonstrates definite sclerotic changes on plain radiographs, with no alteration in the size or shape of the lunate. Additionally, one or more fracture lines may be present.

In stage III, the entire lunate collapses. Later, stage III is divided into stages IIIA and B [33]. In stage IIIA, lunate collapse occurs, but carpal height and alignment remain normal. Stage IIIB has lunate collapse with fixed scaphoid rotation, proximal capitate migration, and loss of carpal height. As the carpal height ratio decreases, the lunate collapses, and the capitate migrate proximally. Scaphoid rotation produces a dorsal intercalated segment instability (DISI) pattern of carpal instability. In stage IV, continued carpal collapse is related to arthritic changes in the radiocarpal and midcarpal joints. Radiographs show subchondral sclerosis with joint space narrowing, osteophyte formation, and degenerative cysts.

Table 6.1 Lichtman osseous classification of Kienböck's disease [36] (引用番号)

Stage	Radiographic findings	MRI findings
I	Normal	T1: decreased, T2: variable
II	Lunate sclerosis	T1: decreased, T2: variable
IIIA	Lunate collapse + normal carpal alignment	T1: decreased, T2: variable
IIIB	Lunate and carpal collapse +	T1: decreased, T2: usually decreased
IIIC	Lunate collapse + a coronal fracture/ fragmentation of the lunate	T1: decreased, T2: variable
IV	Lunate collapse + radiocarpal/midcarpal arthritis	T1: decreased, T2: decreased

Stages 0 and IIIC were included in the latest version of the classification [34]. Stage 0 represents the onset of lunate ischemia; patients in stage 0 may have a normal MRI. Lichtman himself described that stage 0 is hypothetical. Therefore, there is no specific test to diagnose stage 0 objectively. Stage IIIC is defined as a complete coronal plane split, regardless of the lunate or wrist morphology. This modification was made because patients with a complete coronal split of the lunate tend to have a poor prognosis. Lichtman himself described the classification as the Lichtman osseous classification in his latest review and did not include stage 0 [36].

The reliability or the reproducibility of the Lichtman classification has been studied in several reports [37, 38]. Jensen et al. investigated the reliability of the unmodified four-stage Lichtman classification with four observers for 76 radiographs [37]. They reported reliability kappa values ranging from 0.45 to 0.52 and reproducible kappa values ranging from 0.26 to 0.63. Jafarnia et al. also investigated the reliability of a nonmodified four-stage Lichtman classification with four observers [38]. They reported reliability kappa values ranging from 0.66 to 0.74 and reproducible kappa values ranging from 0.72 to 0.82. There was no statistically significant difference in reliability or reproducibility among the observers with different amounts of experience in hand surgery. Goldfarb et al. proposed a modification to the classification system in which stage IIIB was defined as a radioscaphoid angle greater than 60° [22]. With this modification, interobserver reliability increased from a kappa value of 0.63–0.75. Goeminne et al. also reported good reliability and reproducibility of the classification [39]. They reported reliability kappa values of 0.52–0.77 and reproducible kappa values of 0.72–0.90 among four observers who reviewed radiographs from 70 patients. Contrary to the above three studies, Aydemir et al. reported poor reliability among 10 residents, 10 orthopedic surgeons, and 10 hand surgeons [40]. They reported a reliability kappa value of 0.203 within all of the observers. They concluded that the Lichtman classification by plain radiographs alone is insufficient and should be supported by other imaging and measurement techniques.

Schmitt et al. reported how gadolinium perfusion enhanced T1-weighted fast spin–echo (FSE) fat-saturated sequences [29]. Gadolinium enhancement assists with distinguishing necrotic parts from neovascular repair tissue with high signal. They classified the lunate signal alterations after administration of intravenous gadolinium contrast into four stages: MRI stage N, normal; MRI stage A, ischemic (viability maintained); MRI stage B, partially necrotic (viability partially lost); and MRI stage C, completely necrotic.

Bain et al. reported an arthroscopic assessment and classification of Kienöck's disease [41], in which articular surfaces of the lunate were diagnosed as functional or nonfunctional arthroscopically. A functional articular surface has a smooth appearance and is firm to palpation, while a nonfunctional articular surface has at least one of the following findings: extensive fibrillation, fissuring, localized or extensive loss, a floating articular surface, or fracture.

References

1. Kienböck R. Über traumatische Malazie des Mondbeines und ihre Folgezustände: Entartungsformen und Kompressionsfrakturen. Fortschritte auf dem Gebiet der Roentgenstrahlen. 1910;16:78–103.
2. Lichtman DM, Mack GR, MacDonald RI, Gunther SF, Wilson JN. Kienböck's disease: the role of silicone replacement arthroplasty. J Bone Joint Surg Am. 1977;59(7):899–908.
3. Epner RA, Bowers WH, Guilford WB. Ulnar variance--the effect of wrist positioning and roentgen filming technique. J Hand Surg Am. 1982;7(3):298–305.
4. Kristensen SS, Thomassen E, Christensen F. Ulnar variance in Kienböck's disease. J Hand Surg (Edinburgh, Scotland). 1986;11(2):258–60.
5. Nakamura R, Tanaka Y, Imaeda T, Miura T. The influence of age and sex on ulnar variance. J Hand Surg (Edinburgh, Scotland). 1991;16(1):84–8.
6. Schuind FA, Linscheid RL, An KN, Chao EY. A normal data base of posteroanterior roentgenographic measurements of the wrist. J Bone Joint Surg Am. 1992;74(9):1418–29.
7. Gelberman RH, Salamon PB, Jurist JM, Posch JL. Ulnar variance in Kienböck's disease. J Bone Joint Surg Am. 1975;57(5):674–6.
8. Thienpont E, Mulier T, Rega F, De Smet L. Radiographic analysis of anatomical risk factors for Kienböck's disease. Acta Orthop Belg. 2004;70(5):406–9.
9. Coleman DA, Blair WF, Shurr D. Resection of the radial head for fracture of the radial head. Long-term follow-up of seventeen cases. J Bone Joint Surg Am. 1987;69(3):385–92.
10. Palmer AK, Glisson RR, Werner FW. Ulnar variance determination. J Hand Surg Am. 1982;7(4):376–9.
11. Yoshida T, Tada K, Yamamoto K, Shibata T, Shimada K, Kawai H. Aged-onset Kienböck's disease. Arch Orthop Trauma Surg. 1990;109(5):241–6.
12. Steyers CM, Blair WF. Measuring ulnar variance: a comparison of techniques. J Hand Surg Am. 1989;14(4):607–12.
13. D'Hoore K, De Smet L, Verellen K, Vral J, Fabry G. Negative ulnar variance is not a risk factor for Kienböck's disease. J Hand Surg Am. 1994;19(2):229–31.
14. Bonzar M, Firrell JC, Hainer M, Mah ET, McCabe SJ. Kienböck disease and negative ulnar variance. J Bone Joint Surg Am. 1998;80(8):1154–7.
15. Afshar A. Kienböck disease in the skeletally immature patient. J Hand Surg Am. 2018;43(5):465–9.
16. Muramatsu K, Ihara K, Kawai S, Doi K. Ulnar variance and the role of joint levelling procedure for Kienböck's disease. Int Orthop. 2003;27(4):240–3.
17. Tsujimoto R, Maeda J, Abe Y, et al. Epidemiology of Kienböck's disease in middle-aged and elderly Japanese women. Orthopedics. 2015;38(1):e14–8.
18. Tsuge S, Nakamura R. Anatomical risk factors for Kienböck's disease. J Hand Surg (Edinburgh, Scotland). 1993;18(1):70–5.
19. Mirabello SC, Rosenthal DI, Smith RJ. Correlation of clinical and radiographic findings in Kienböck's disease. J Hand Surg Am. 1987;12(6):1049–54.
20. Youm Y, Flatt AE. Kinematics of the wrist. Clin Orthop Relat Res. 1980;149:21–32.
21. Gilula LA, Weeks PM. Post-traumatic ligamentous instabilities of the wrist. Radiology. 1978;129(3):641–51.
22. Goldfarb CA, Hsu J, Gelberman RH, Boyer MI. The Lichtman classification for Kienböck's disease: an assessment of reliability. J Hand Surg Am. 2003;28(1):74–80.
23. Condit DP, Idler RS, Fischer TJ, Hastings H 2nd. Preoperative factors and outcome after lunate decompression for Kienböck's disease. J Hand Surg Am. 1993;18(4):691–6.
24. Arnaiz J, Piedra T, Cerezal L, et al. Imaging of Kienböck disease. AJR Am J Roentgenol. 2014;203(1):131–9.

25. Viegas SF, Wagner K, Patterson R, Peterson P. Medial (hamate) facet of the lunate. J Hand Surg Am. 1990;15(4):564–71.
26. Tatebe M, Imaeda T, Hirata H. The impact of lunate morphology on Kienböck's disease. J Hand Surg Eur Vol. 2015;40(5):534–6.
27. Rhee PC, Jones DB, Moran SL, Shin AY. The effect of lunate morphology in Kienböck disease. J Hand Surg Am. 2015;40(4):738–44.
28. Friedman L, Yong-Hing K, Johnston GH. The use of coronal computed tomography in the evaluation of Kienbock's disease. Clin Radiol. 1991;44(1):56–9.
29. Schmitt R, Heinze A, Fellner F, Obletter N, Strühn R, Bautz W. Imaging and staging of avascular osteonecroses at the wrist and hand. Eur J Radiol. 1997;25(2):92–103.
30. Mohan A, Knight R, Ismail H, Trail IA. Radiographic and computed tomography correlation of Kienböck's disease: is there a need to revisit staging with improved imaging? J Wrist Surg. 2020;9(1):39–43.
31. Stahl F. On lunatomalazia (Kienböck's disease): a clinical und roentgenological study, especially on its pathogenesis and the late results of immobilization treatment. Acta Chir Scand Suppl. 1947;126:1–133.
32. Decoulx P, Marchand M, Minet P, Razemon JP. Kienbock's disease in miners; clinical & pathogenic study with analysis of 1330 x-rays of the wrist. Lille Chir. 1957;12(2):65–81.
33. Lichtman DM, Degnan GG. Staging and its use in the determination of treatment modalities for Kienböck's disease. Hand Clin. 1993;9(3):409–16.
34. Lichtman DM, Lesley NE, Simmons SP. The classification and treatment of Kienbock's disease: the state of the art and a look at the future. J Hand Surg Eur Vol. 2010;35(7):549–54.
35. Lichtman DM, Pientka WF 2nd, Bain GI. Kienbock disease: moving forward. J Hand Surg Am. 2016;41(5):630–8.
36. Lichtman DM, Pientka WF 2nd, Bain GI. Kienbock disease: a new algorithm for the 21st century. J Wrist Surg. 2017;6(1):2–10.
37. Jensen CH, Thomsen K, Holst-Nielsen F. Radiographic staging of Kienböck's disease. Poor reproducibility of Ståhl's and Lichtman's staging systems. Acta Orthop Scand. 1996;67(3):274–6.
38. Jafarnia K, Collins ED, Kohl HW 3rd, Bennett JB, Ilahi OA. Reliability of the Lichtman classification of Kienböck's disease. J Hand Surg Am. 2000;25(3):529–34.
39. Goeminne S, Degreef I, De Smet L. Reliability and reproducibility of Kienbock's disease staging. J Hand Surg Eur Vol. 2010;35(7):555–7.
40. Aydemir AN, Yücens M, Cansu CE, Demirkan AF. Are plain radiographs reliable in Lichtman classification? Jt Dis Relat Surg. 2020;31(1):34–8.
41. Bain GI, Begg M. Arthroscopic assessment and classification of Kienbock's disease. Tech Hand Up Extrem Surg. 2006;10(1):8–13.